VARIABLE CONDUCTANCE THERMAL CONTROL BY PASSIVE OR ACTIVE CONTROL OF FLUID MANIPULATION

A.A.M. Delil
Advanced Aerospace Thermal Control Systems Consultant
Kaspischestraat 13, 8303 EX Emmeloord, Netherlands
Phone: +31 527617576, Fax: +31 847218374 (receiving only), E-mail: adelil@zonnet.nl

Abstract

This keynote paper presents a concise survey of the international research carried out for developing spacecraft oriented (variable conductance) two-phase thermal control systems, based on passive or active control of fluid manipulation. It focuses on variable conductance heat pipes, based on a control using non-condensable gas. It illustrates the historical development and arguments why these relatively simple two-phase thermal control systems are the preferred solution to meet the different restrictions induced by the requirement specifications of many, relatively low power (say up to 1 kW) applications space. The paper briefly revisits alternative control approaches, considered in the past. It also discusses a novel approach, currently being investigated.

KEYWORDS

Spacecraft, Passive Thermal Control, Active Thermal Control, Variable Conductance Heat Pipe, Capillary Pumped Loop, Loop Heat Pipe, Vapour Pressure Driven Loop, Mechanically Pumped Loop, Two-Phase Thermal Bus, Electro-Osmosis, Electro-Hydro-Dynamics, Thermal Modelling. Electric Wetting Control.

INTRODUCTION

Passive two-phase thermal control devices have either no or only limited thermal control capabilities to guarantee a desired almost constant temperature set-point of a heat source (sensor, electronic box, evaporator, etc.), for large variations in heat load or large heat sink condition excursions. This limited passive thermal control capability is briefly discussed for a Variable Conductance Heat Pipe (VCHP), Loop Heat Pipe (LHP) and a Vapour Pressure Driven Loop (VPDL).

Active control of two-phase thermal control devices delivers this almost constant temperature set-point task, via condenser blocking: By feedback control of the temperature in the non-condensable gas reservoir of a VCHP and control of the fluid inventory of two-phase loops. The latter is usually realised by feedback control of the loop reservoir temperature: Increasing the reservoir temperature (hence the vapour saturation temperature) forces liquid out of the reservoir into the loop, decreasing the reservoir temperature forces liquid from the loop back into the reservoir.

The pumping pressure in capillary pumped systems is limited, meaning that they can't be used in large power two-phase thermal control systems: Above say 5 kW one must use a mechanical pump in the liquid section of loop, hence a Mechanically Pumped Loop (MPL), also called thermal bus. A thermal bus can be in a series or in a parallel configuration, each one having advantages/drawbacks. One drawback of any MPL consists of the vibrations induced by the mechanical liquid pump. This implies that for spacecraft systems that do not allow such vibrations, one prefers capillary pumping or an alternative, no vibrations producing, pumping mechanism. Therefore it will be discussed that one tried and is still trying to develop novel alternative systems, based on electro-osmotic or electro-hydrodynamic pumping, or on capillary pumping combined with electric liquid manipulation.

Finally it is remarked that many detailed descriptions of the merits and terrestrial and in-flight performances of CPL, LHP, VPDL and MPL can be found in the text and references of [1-3].

VARIABLE CONDUCTANCE HEAT PIPES

Variable conductance issues

VCHP differ from normal HP by their thermal control capability: To keep set-point temperature of a heat source (mounted on the evaporator) almost constant, independent of changes of the boundary conditions (i.e. the by the source dissipated power and condenser heat sink temperature).

Methods to achieve VCHP behaviour are [4, 5]:

- Condenser blocking by non-condensable gas, the so-called gas-loaded VCHP, schematically shown in Fig. 1 [4, 5]**.** The gas is swept by the moving vapour towards the condenser end, where it forms a gas plug that blocks part of the condenser area for conducting heat to the sink. The size of this plug, yielding the variable conductance, depends on the thermal loading and the pressure in the gas reservoir, usually (but not necessarily) located at the condenser end (Fig. 2). This pressure, hence the plug size, can be controlled (e.g. in a active feedback way) by controlling the temperature of the gas in the reservoir (using a heater and a cooler, e.g. a Peltier element), the gas inventory (using a control valve and an additional gas reservoir), or the reservoir size (by a bellows system), the so-called variable reservoir volume gas-controlled VCHP (Fig. 3).
- Condenser flooding, using excess liquid to vary the active condenser area.
- Liquid flow control by interrupting or impeding the return of the condensate in the wick. For dissipative heat sources this means just providing "on-off" control, i.e. thermal switching.
- Vapour flow control by interrupting or throttling the vapour flow between the heat pipe evaporator and condenser, which gives rise to the pressure difference, hence the temperature difference, between these regions, meaning variable conductance.

The most viable VCHP is of the gas-buffered (gas-loaded) type, equipped with a cold reservoir (without or with a capillary wick), or with a hot reservoir [4, 5]. Their thermal control properties turn out to be limited in case of passive control, even in case of passive control of a VCHP equipped with a bellows reservoir [4]: Perfect temperature control can only be realised using (active) electrical feedback control. [4, 5] yield a comparison between the various configurations, showing the advantages and drawbacks of the various options. Aspects of working fluid selection and reservoir sizing and location within or outside the VCHP are also discussed, including feedback control issues.

The prediction of VCHP control behaviour depends on the particular thermal model used. Mostly this can be done using the Edwards-Marcus flat front model [4]. But for some VCHP applications, especially those requiring a VCHP with a low-vapour-pressure working fluid, inertial effects (that can occur for instance during start-up) were to be included in the model. The model, developed at NLR to account for inertia and friction [5, 8-13], and its typical modelling outcomes, illustrate the impact of these effects for designing (active) feedback thermal control systems: Differences for designing a control system, using the Edwards-Marcus model or the NLR model, can be substantial.

The Edwards Marcus Model for a Gas-Loaded VCHP

The commonly used Edwards-Marcus model is physically incomplete, but ideal to illustrate the working principle, governing parameters, sensitivity for parameter variations, and so on. The discussion is restricted to a VCHP with a cylindrical cross-section, assuming the vapour to obey the Clausius-Clapeyron equation and the gas to obey the ideal gas law. Other equations, derived in [4], are not given here, as they can simply be obtained by setting inertia and friction terms in the NLR model equations equal to zero. Fig. 4 schematically shows a gas-loaded VCHP, and the temperature distribution according to the Edwards-Marcus flat front model, which assumes a sharp vapour-gas interface. This is realistic as diffuse front model calculations showed that the diffusion effect is negligible compared with friction/inertia effects [6, 9, 10]. The Edwards-Marcus model assessed (details are in [4]): The effect of a fixed sink temperature, the effect of sink temperature variations, the effect of working fluid for fixed and variable sink conditions, wicked cold reservoir issues (both for $T_R \neq T_S$ and $T_R = T_S$) and non-wicked cold reservoir issues, reservoir sizing, limitations of passive control, realisation of a variable set-point by keeping the gas inventory constant and varying the reservoir volume (using an internal/external bellows system), and issues of feedback controlled VCHP (FCHP), which includes an external feedback control loop. Interesting results (Figs. 5-9) are:

- Like for passive VCHP, FCHP control means that the maximum reservoir temperature must be equal to or below the evaporator temperature, to prevent that the reservoir becomes an evaporator.
- Unlike it is the case in a passively controlled VCHP, the FCHP allows to lower the evaporator temperature for increasing heat input. Consequently the actively controlled FCHP yields a much closer heat source temperature control than a passive system does.
- Methanol is superior to ammonia for passively controlled VCHP, ammonia is superior to methanol in the heated wicked reservoir FCHP.

Further information on FCHP steady-state and transient performance can be found in [7, 8].

The NLR Improved Model

As said, the Edwards-Marcus model is physically incomplete. Therefore NLR developed an improved transient model [9-13], being easily implemented in existing general thermal analyser computer programs. The model accounts for the following effects: Radial thermal conduct ion in the wall and wick of the heat pipe and effects of friction and inertia in the moving vapour. Using this model it has been shown that inertial effects can be considerable in that part of the heat pipe operating range that is characterised by low vapour pressures. This turns out to be a rather wide range for heat pipe working fluids with relatively low vapour pressures, such as methanol, ethanol and the liquid metals. For other working fluids this range is only a narrow one, close to the freezing point [9-15]. Since the net effect of friction is increasing the velocity of a subsonic flow, friction enhances the impact of inertial effects and it widens the above-mentioned operating range. Friction also lowers the sonic limitation to the heat transport capability making a heat pipe more sensitive for blocking of the heat transport by choking [15, 16]. In the condenser section inertia decelerates the vapour flow leading to temperature and pressure increase. Friction counteracts this by accelerating the vapour flow. Usually the effects of inertia dominate frictional effects. However, operating conditions have been identified where frictional effects are dominant, especially for front positions far from the condenser entrance. In these situations small variations in thermal loading yield very large front displacements, accompanied by transfer functions unfavourable for (feedback) control systems.

Calculations were performed with the computer program based on the current model. The results of these calculations are used: To design a VCHP for the experimental verification of the model developed, to define test schemes and proper test conditions to predict VCHP transfer functions for control purposes, and to identify possible problems with respect to performance and control limits.
Since the aforementioned calculations are straightforward and easy to perform, implementation of the NLR model in existing thermal analyser programs for spacecraft was relatively simple and was realised after completing the model with axial conduction. The complete model constitutes an adequate basis for modelling the behaviour of a gas-loaded VCHP at reasonable costs.

The following restrictions and assumptions apply for the calculated results presented below:

- The model is uniaxial and applicable to cylindrical VCHP's only, in other words for VCHP's with homogeneous or axially grooved wicks, but the results obtained for the cylindrical configuration contribute to understand the performance of more complicated configurations.
- Only steady-state conditions are considered, axial conduction by wall/wick is not taken into account.
- The radial heat transfer per unit of condenser (evaporator) area is proportional to the difference between vapour temperature and sink (source) temperature. This means that the radial conduction properties do not depend on the temperature, which is valid for not too large temperature intervals.
- Diffusion is set zero, since its effects have been shown to be negligible compared with inertial effects [12, 13]. The vapour has a constant viscosity and obeys the Clausius-Clapeyron relation :

$$\rho_v = \alpha\, M_v/(R_0\, T) \exp(-N_S/T), \tag{1}$$

α is a reference pressure. N_S is a control sensitivity factor, useful to rank working fluids[4]:

$$N_S = (h_{lv}\, M_v/(R_0), \tag{2}$$

The governing model equations can be written as [12, 13]:

$$\begin{pmatrix} \frac{\rho_v}{M_v} & u & 0 \\ \beta\rho_v u & R_0 T & \frac{R_0\rho_v}{M_v} \\ 0 & \frac{M_v}{\rho_v} & -\frac{N_s}{T^2}+\frac{1}{T} \end{pmatrix} \begin{pmatrix} \frac{du}{dx} \\ \frac{1}{M_v}\frac{d\rho_v}{dx} \\ \frac{dT}{dx} \end{pmatrix} = \begin{pmatrix} -\frac{Q_i}{A_c h_{lv} M_v} \\ -\frac{2f\rho_v u^2}{d}+\frac{uQ_i}{A_c h_{lv}}\left(\dot{\beta}-\gamma'\right) \\ 0 \end{pmatrix} \tag{3}$$

These equations are the constitutive equations for compressible fluid flow integrated over the cross-sectional area [17], and the differential form of the Clausius-Clapeyron relation . Q_i (or Q) is the heat input. β is the shape (flow profile) factor for the velocity profile, varies from 1 for pure plug flow to 4/3 for pure laminar flow. Friction factor f can be approximated by [17] f = 16/Re for laminar flow (Re

< 2000) or $f = 0.079/(Re)^{1/4}$ for turbulent flow (Re > 2000), with Reynolds number $Re = p_v u d/\mu_v$. The hydraulic diameter d equals 4 times the ratio between cross-sectional area and perimeter. Friction factors f for heat pipes can be up to 3 times larger than the smooth pipe values [14]. γ' accounts for the transition of radial to axial momentum. It is assumed to be negligible for Re < 2000, and is for Re > 2000 approximated by $\gamma' = 1 - 2000/Re$. The heat input per unit length is written: $Q_i = B\,(T_{SO} - T)$ in the evaporator ($0 \le x \le L_E$), $Q_i = 0$ in the adiabatic section ($L_E \le x \le L_E + L_A$) and $Q_i = A\,(T - T_S)$ in the condenser ($L_E + L_A \le x \le L_E + L_A + L_C$). The total heat throughput is obtained by integrating Q_i

$$Q = \int Q_i\,dx = \int_{LE+LA}^{LE+LA+LC} A\,(T - T_S)dx = \int_{0}^{LE} B\,(T_{SO} - T)dx. \qquad (4)$$

Additional relations are the equations of state for the vapour $P_v = (\rho_v/M_v)\,R_0\,T_v$ and for the control gas $p_g = (\rho_g/M_g)\,R_0\,T_g$). Finally it is remarked that u = 0 at the flat front position x_f where the temperature is discontinuous i.e. equal to T_f at the upstream side and T_S at the downstream side. The pressure is continuous in the entire VCHP. Consequently pressure equilibrium yields the gas control relation and the molar gas content

$$p_g = (\rho_g/M_g)\,R_0\,T_S = \alpha\,[\exp(-N_S/T_f) - \exp(-N_S/T_S)], \qquad (5)$$

$$n_g/M_g = (\alpha A_C/R_0 T_S)(L_E + L_A + L_C - x_f)\,[\exp(-N_S/T_f) - \exp(-N_S/T_S)] + (\alpha V_R/R_0 T_R)\,[\exp(-N_S/T_f) - \exp(-N_S/T_S)]. \qquad (6)$$

Equation (3) becomes singular if and only if the determinant of the 3x3 matrix is zero. This is equivalent with a critical velocity

$$u_s = [\{N_S/(N_S - T)\}\ \{R_0\,T/(\beta\,M_v\}]^{1/2} \qquad (7)$$

being the velocity of sound $(\partial p_v/(\partial \rho_v)^{1/2}$, as it straightforwardly follows from the equation of state for the vapour and the Clausius-Clapeyron relation. The corresponding sonic heat throughput limit is:

$$Q_s = \rho_v\,A_C\,h_{lv}\,u_s = [\{N_S/(N_S - T)\}\ \{R_0\,T/(\beta\,M_v\}]^{1/2}\,(\alpha\,A_C\,N_S)\exp(-N_S/T). \qquad (8)$$

NLR Modelling Results

Various calculations have been carried out in order to define a test heat pipe and test conditions for the experimental verification of the model. A correct definition of the VCHP and the test conditions will yield detectable frictional and inertial effects. In addition requirements for easy experimenting, preferably not too far from room temperature, must be met. Based on these requirements and on the results of calculations, a SABCA M96-like VCHP was selected [12, 13], with methanol as the working fluid (properties are in [18, 19]). HP characteristics: Outer diameter 9.5 mm, SS wall thickness 0.5 mm, composite wick of one circumferential mesh layer and a central 8-shaped mesh filled artery ($A_v = 2.6*10^{-5}$ m^2 , d = 2.03 mm), evaporator length 0.1 m. Results of calculations for this heat pipe are discussed below. A VCHP with these characteristics was built at NLR to verify the outcomes of the calculations This VCHP and the experimental results have been published [20].

Fig. 10 shows an example of calculated temperature and vapour velocity distributions along the pipe. It illustrates the accelerating effect of friction, which especially at higher throughputs values leads to performances (front positions, front temperatures), which considerably differ from the corresponding zero-friction performances. This clearly leads to differences in transfer functions. The figure also illustrates that in the condenser friction becomes dominant at the highest throughput values only. For lower throughput inertia dominates friction (temperature and pressure recovery). Finally it is remarked that the accelerating effect of friction is accompanied by a vapour temperature decrease: It limits the maximum throughput for given source and sink conditions, since the vapour temperature at the condenser entrance must be higher than the sink temperature.

Choking, occurring when the local vapour velocity reaches the velocity of sound, limits the heat pipe throughput. In models neglecting friction choking adjusts the maximum throughput for conditions pertaining to the evaporator exit, where the vapour flow reaches its maximum velocity and the velocity of sound its minimum value. When friction is taken into account choking can take place in every heat pipe section, depending on the various thermal-loadings. This is illustrated in Fig. 11. In all cases, however, friction lowers the sonic limitation of the heat throughput.

More results of iterative calculations with the computer program developed are in the Figs.12 to16.

They quantify the substantial maximum throughput reduction caused by friction. From Fig.12, illustrating the flow profile factor S impact, it can be concluded that - for the heat pipe selected - the outcomes hardly depend on S if friction is taken into account. As Reynolds numbers turn out to be relatively small at the-low pressure side of the operating range, 4/3 is the β-value to be preferred in further calculations. Fig. 13 illustrates the influence of the sink temperature.

As it has been remarked already, friction accelerates a subsonic flow. Consequently the length of the adiabatic section will influence the maximum heat throughput, as illustrated by Fig.14. The reduction of the throughput caused by friction, already substantial if there is no adiabatic section at all, strongly increases with increasing length of this section. It also has been remarked that friction values for wicked heat pipes might be up to three times the smooth pipe values. The impact of such a higher friction value is shown in Fig.15.

All calculations presented were carried out using a value of 82 W/(m·K) for the equivalent radial conductance in evaporator and condenser. This value was derived from heat pipe material properties, dimensions and a heat transfer coefficient of 4000 W/(m^2·K), a value often used in literature. However, especially in the evaporator, the heat transfer coefficients hence the equivalent radial conductance B can be much smaller. Fig. 16 illustrates how important it is to know this conductance accurately.

Feedback Control Issues

As it is remarked in the introduction, the control of the source temperature for varying thermal loading conditions is possible by actively adjusting the control gas pressure by influencing the reservoir quantities: size or temperature or molar gas content. Fig.17 presents the basic schematic of the feedback control system considered Since the gas pressure p is a function of the throughput Q, the sink temperature T_S and the source temperature T_{SO} one can write

$$dp_g = (\partial p_g/\partial Q)dQ + (\partial p_g/\partial T_S)dT_S + (\partial p_g/\partial T_{SO})\, dT_{SO} \qquad (9)$$

The important transfer functions that can be identified, $(\partial p_g/\partial Q)$, $(\partial p_g/\partial T_S)$, and $(\partial p_g/\partial T_{SO})$, can be determined from relations between Q, x_f and T_f for combinations of constant T_{SQ} and T_S and between T_S, x_f, T_f for combinations of constant T_S and Q. Fig. 18 presents, as an example, the relation between the gas pressure and the heat throughput for some source/sink temperature combinations. The derivative of the curves is the transfer function $(\partial p_g/\partial Q)$. From this figure it can be concluded that the strong non-linearity for higher throughput values may lead to instabilities, considerably complicating the design of the control system, and may limit the operating range of the system. The differences between the curves derived for the Edwards-Marcus model, which neglects friction and inertia, and the corresponding curves derived according to the NLR model, clearly illustrate the importance of the model for the determination of the parameters of the feedback control system.

Finally it is remarked that for designing passive control systems, using a VCHP with fixed reservoir size, temperature and gas content, the curves are used to predict the magnitude of source temperature variations induced by variations in thermal loading.

TWO-PHASE THERMAL CONTROL SYSTEMS, OTHER THAN VCHP

Active (condenser flooding) control of a VPDL (Fig. 19) yields periodical set-point temperature variations, as the evaporator vapour pressure (temperature) has to rise to open a pre-set valve. After opening, the pressure (evaporator temperature) will drop until the valve closes, and the process will be repeated. The result is a periodic variation around set-point temperature. Its frequency changes with variations in heat load. The bandwidth of the oscillation depends on the steepness of the dp_v/dT curve of the working fluid used (Fig. 20) around the set-point. A passive device can give similar control, only if the sink temperature remains constant.

A Loop Heat Pipe (LHP), which normally operates in the constant conductance mode, is able to operate also in a variable conductance mode, under very limited conditions. Without going into detail one can easily see the variable conductance mode of the LHP, when looking at the typical performance graphs of the GLAS heat pipe (Fig. 21), showing evaporator temperature versus the heat throughput for the two extreme cases, being a high superheat start-up and a low superheat start-up. Both curves have a minimum, meaning that starting from the left side, an increase of heat input power will lead to a decrease of the evaporator temperature till the minimum will be reached. Further increase of input power will cause an increasing evaporator temperature, entering the LHP constant conductance mode,

in which evaporator temperature increases/decreases almost linear with power. This means variable conductance behaviour around the minima, as there dT_E/dQ changes sign.

CONTROL ALTERNATIVES, RECOMMENDED TO BE INVESTIGATED

In the past was the choice straightforward: The gas-reservoir controlled VCHP and the liquid reservoir content controlled condenser flooding in CPL, LHP, VPDL and MPL are the best options for most applications. This will be valid in the future, but doesn't mean that the alternatives (dropped in the past) and novelties are of interest to be looked at for special applications. Alternatives are ongoing, being the reassessment of the vapour throttling approach (many years proposed and tested by Sundstrand Inc. for MPL) for VCHP, liquid condenser flooding in VCHP, the electro-osmotic VCHP [21], EHD control of heat pipes and two-phase loops [22], and the electric wetting phenomenon [23]. Electric wetting means "dancing droplets" [24], being the on/off switching of a low electric voltage to locally change a flowing liquid layer pattern in a liquid sphere, that interrupt/stops the flow. The HP application of electric wetting is being investigated (by the author of this keynote), as it might be of interest for the development of future miniature, low power systems.

CONCLUDING REMARKS

A brief survey is given of research on spacecraft oriented variable conductance two-phase thermal control systems based on passive or active control of fluid manipulation, focusing on gas-loaded VCHP. It was illustrated why these relatively simple two-phase thermal control systems are the preferred solution to meet the different restrictions induced by the requirement specifications of many, relatively low power (say up to 1 kW) applications space. Alternative control approaches, considered in the past or new ones, are mentioned.

ABBREVIATIONS AND SYMBOLS

CPL Capillary Pumped Loop(s)
EHD Electro-Hydro-Dynamic(s)
EO Electro-Osmotic
HP Heat Pipe(s)
LHP Loop Heat Pipe(s)
MPL Mechanically Pumped Loop(s)
NLR Dutch National Aerospace Laboratory
VCHP Variable Conductance Heat Pipe(s)
VPDL Vapour Pressure Driven Loop(s)

A,B equivalent thermal conductance (W/(m·K))
A' heat transfer area per unit length (m)
d hydraulic diameter (m)
f friction factor
h heat transfer coefficient ($W/(m^2 \cdot K)$)
h_{lv} latent heat of vaporisation (J/(kmol·K))
L length (m)
N_S gas control sensitivity factor (K or °R)
M molecular weight (kg/kmol, lb /lbmole)
p pressure (N/m^2, psi)
Q power, heat load/throughput (W)
R_0 gas constant (J/(K·kmol))
R_u gas constant (Btu/°R lbmole)
Re Reynolds number (-)
T temperature (K, °C or °R, °F)
u vapour velocity (m/s)
V volume (m^3)
x axial co-ordinate (m)

Greek
α reference pressure (Pa, N/m^2, psi)
β shape or flow profile factor
γ latent heat of evaporation (Btu/°R lbmole)
γ' radial-axial momentum transition factor
μ viscosity ($N.s/m^2$)
ρ density (kg/m^3)
Δ difference

Subscripts
A, a adiabatic section
C, c condenser
E, e evaporator
f front
g gas
l liquid
max maximum
min minimum
R reservoir
S, s sink or sonic
SO source
va, v vapour (core)
w wick

References

1. Delil A.A.M. Two-Phase Heat Transport Systems for Thermal Control Applications // *ICHMT short Course on Passive Thermal Control*, Antalya, Turkey, 2003.
2. Delil A.A.M. Oscillating/Pulsating Heat Transfer & Thermal Control Devices (In Acceleration

Environments from Micro- to Supergravity) // *ICHMT Short Course on Passive Thermal Control*, Antalya, Turkey, 2003.
3. Delil A.A.M. Mechanically Pumped Two-Phase Thermal Control Loops // *ICHMT Short Course on Passive Thermal Control*, Antalya, Turkey, 2003.
4. Marcus B.D. Theory and design of variable conductance heat pipes, NASA CR-2018, 1972.
5. Delil A.A.M. Variable Conductance Heat Pipes: Modelling and Applications // *ICHMT Short Course on Passive Thermal Control*, Antalya, Turkey, 2003.
6 Van der Vooren J., Delil A.A.M., Sanderse, A. Uniaxial model for a gas-loaded-variable conductance heat pipe, NLR-TR-80048, 1980.
7. Bienert W., Brennan P., Kirkpatrick J.P. Feedback controlled variable conductance heat pipes, AIAA paper 71-421, AIAA 6th Thermophysics Conference, 1971.
8. Bienert W. & Brennan P. Transient performance of electrical feedback controlled variable conductance heat pipes // ASME paper 71-Av-27, 1971.
9. Van der Vooren, J. & Sanderse A. An improved flat front model for a gas-loaded variable conductance heat pipe // NLR-TR-80049, 1980.
10. Delil A.A.M. & Van der Vooren J. Uniaxial model for gas-loaded variable conductance heat pipe performance in the inertial flow regime // NLR-MP-81010 U // *Advances in heat pipe technology*, Pergamon, Oxford, UK 1989.
11. Van de Wijngaart R. *Uniaxial model for the transient behaviour of the vapour/gas core in a gas-loaded variable conductance heat pipe*, Thesis Delft Technological University, 1982.
12. Delil A.A M & Daniëls H.A.M. Uniaxial model for gas-loaded variable conductance heat pipe performance; The effects of vapour flow friction and inertia, NLR-MP-83058 // *ESA SP 200, Symp. Proc. Environmental and thermal systems for space vehicles*, 1983.
13. Delil A.A.M. Limitations in variable conductance heat pipe performance and control predicted by the current steady state model developed at NLR, NLR-MP-1984-009 // *Proc. 5th International Heat Pipe Conference*, Tsukuba, Japan, 1984. Pp. 225-231.
14. Ivanovskii M.N., Sorokin V.P., Yagodkin I.V. *The Physical Principles of Heat Pipes,* Clarendon Press, Oxford, UK, 1982.
15. Levy E.K. Effects of friction on the sonic velocity limit in sodium heat pipes // AIAA 6th Thermophysics Conference, Tullahoma, USA, 1971.
16. Levy E.K., Chou S.F. The sonic limit in sodium heat pipes // *J. of Heat Transfer Trans. ASME C*, Vol. 6. 1973. Pp. 218-223.
17. Shapiro A. H. *Compressible fluid flow*, RonaId Press Company, New York, 1953.
18. Delil A. A. M. Theory and design of conventional heat pipes for space applications, NLR-TR-77001, 1977.
19. Scrabek E.A., Bienert W.B. NASA Heat pipe design handbook, NASA CR 134264/265, 1972.
20. Van Buggenum R.I.J., Daniels D.H.W. Development, manufacturing and testing of a gas-loaded variable conductance heat pipe // *Proc. 6th Int. Heat Pipe Conference*, Grenoble, France, 1987. Pp. 330-337.
21. Delil A.A.M. Fully controllable heat pipe with a short electro-osmotic pumping section, NLR MP 82049, AIAA 83-317, AIAA Aerospace Sciences Meeting, Reno, USA, 1983.
22. Didion J. Advancements in ElectroHydroDynamic (EHD) Thermal Control Systems // 15th Spacecraft Thermal Control Workshop, El Segundo, USA, 2005. Mugele F. et al. Electrowetting: A convenient way to switchable wettability patterns // J. *Physics: Condensed Matter*, Vol. 17, 2005. Pp. 559-576.
24 Mugele, F., Dancing Droplets, FOM Symposium Flow and Heat, Veldhoven, Netherlands, 2004.

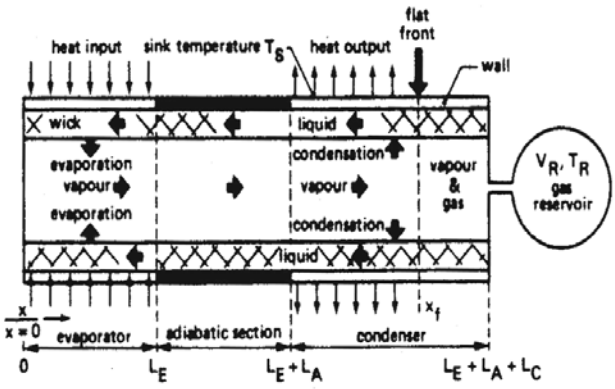

Fig. 1. Schematic of a gas-loaded VCHP, with a wicked or a non-wicked reservoir [13]

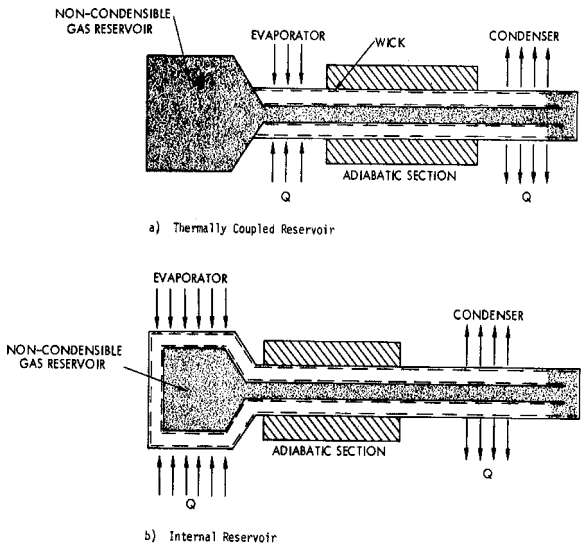

Fig. 2. Hot non-wicked reservoir VCHP (a) Thermally coupled and (b) Internal [4]

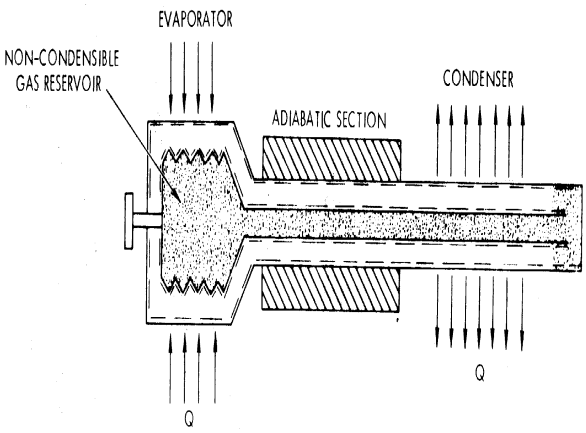

Fig. 3. Schematic of variable reservoir volume gas-loaded VCHP [4]

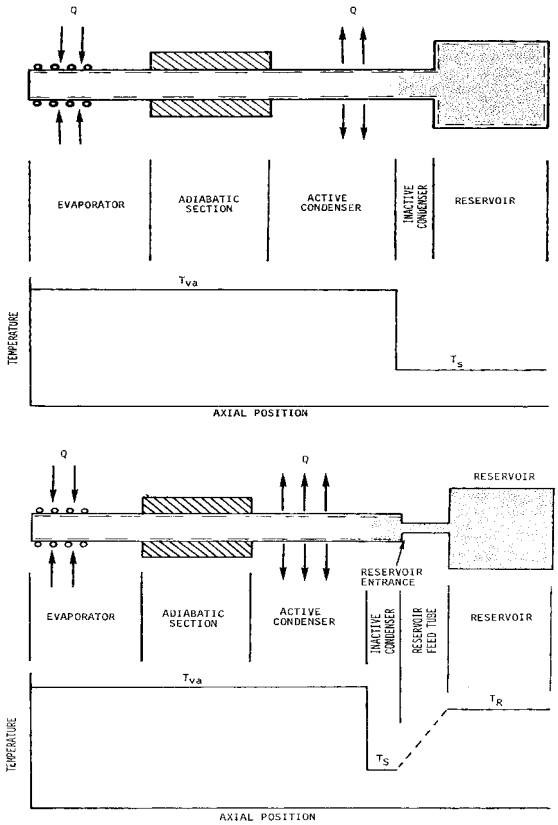

Fig. 4. Schematic flat front T-distribution of a cold wicked (upper figure) and hot non-wicked (lower figure) reservoir gas-loaded VCHP [4]

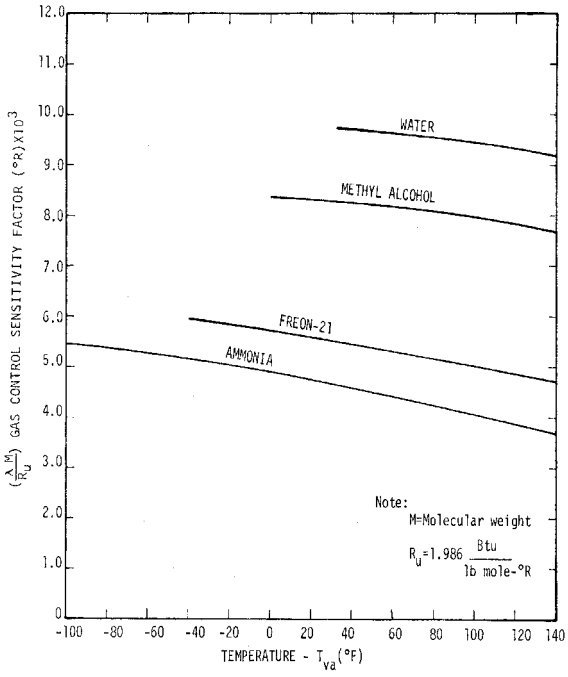

Fig. 5. Gas control sensitivity factor N_S versus temperature for some space-related working fluids [4]

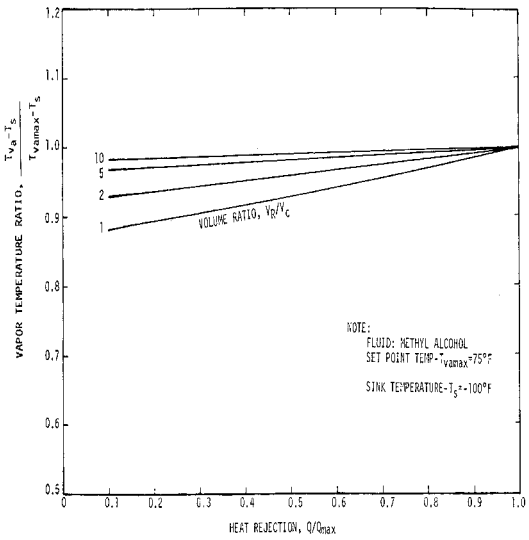

Fig. 6. V_R/V_C effect on control sensitivity, methanol: $T_R = T_s$, $T_{va\ max}$ =38°C, T_s = 22°C [4]

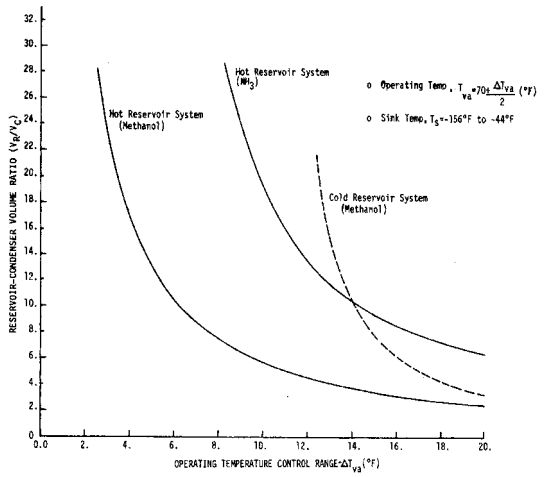

Fig. 7. Reservoir volume requirements versus temperature control range [4]

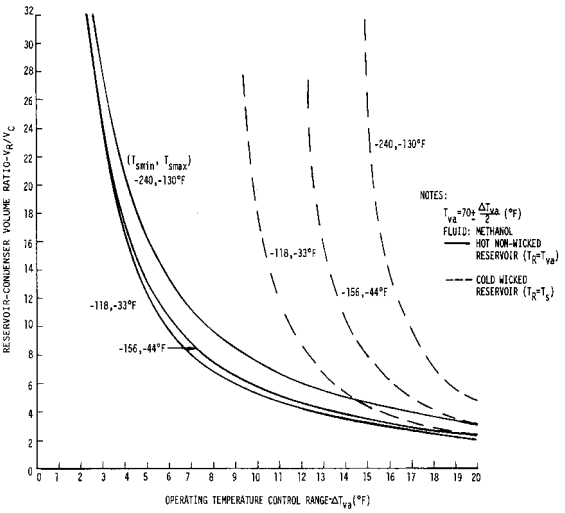

Fig. 8. Reservoir volume requirements versus temperature control range [4]

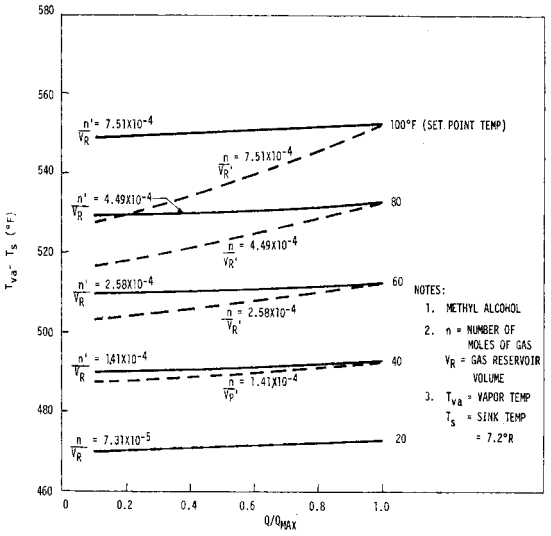

Fig. 9. Comparison of the gas inventory versus reservoir volume [4]

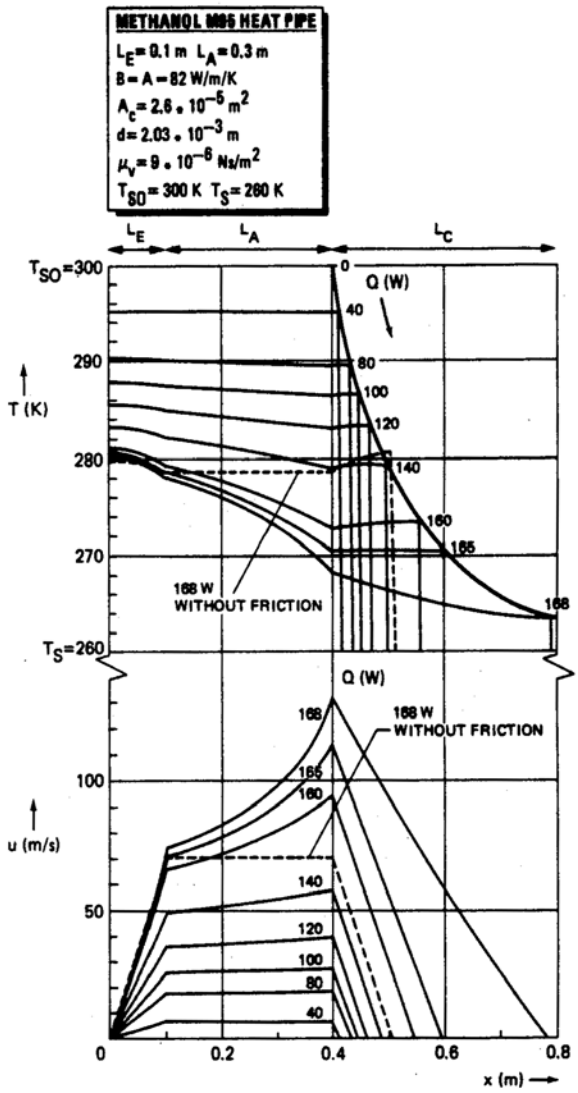

Fig. 10. Vapour velocity and temperature distribution in M95 heat pipe for various throughputs [13].

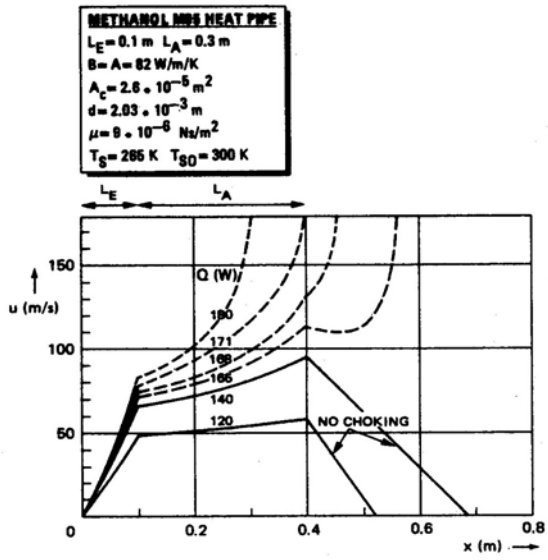

Fig. 11. Choking, for increasing throughput shifts from condenser to adiabatic section [13]

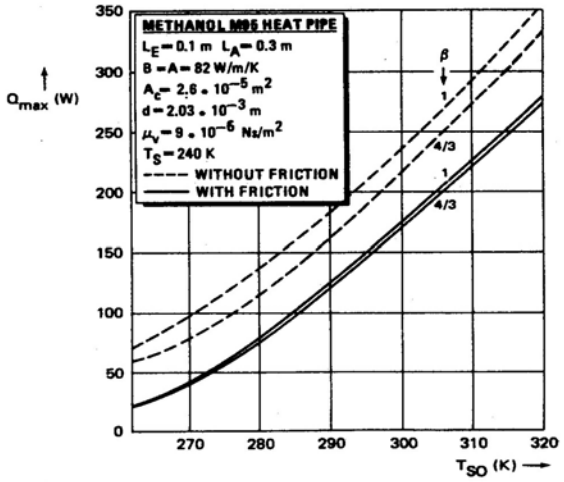

Fig. 12. Maximum power- source temperature,: β=1 Plug flow, β=4/3 laminar [13]

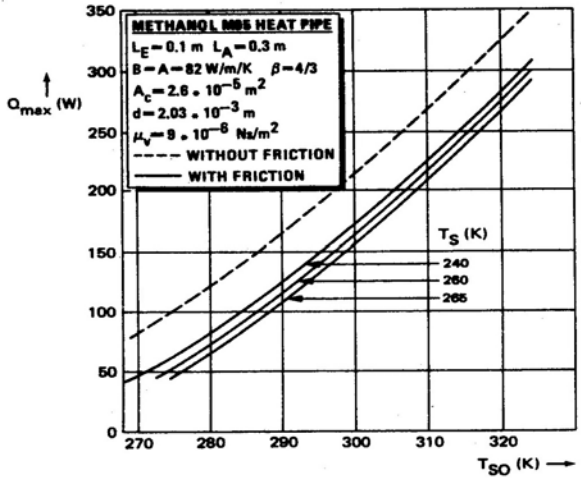

Fig. 13. Maximum throughput versus source temperature, for some sink temperatures [13]

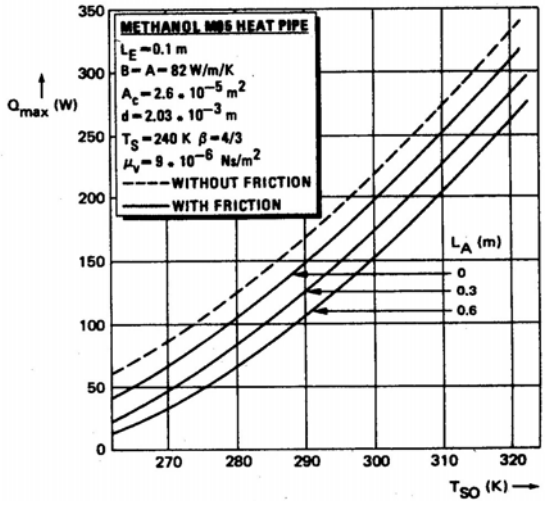

Fig. 14. Maximum throughput versus source temperature for various adiabatic lengths [13]

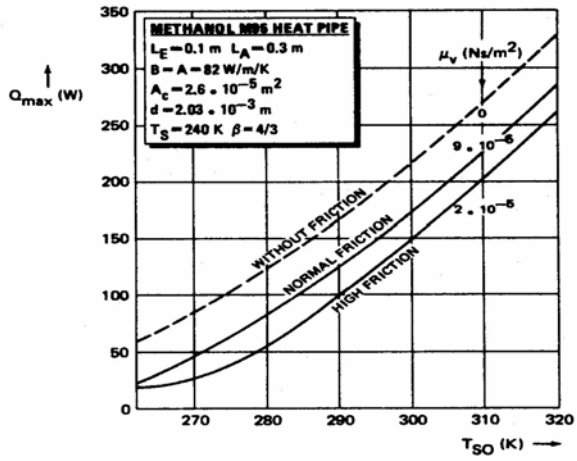

Fig. 15. Maximum throughput versus source temperature for some vapour viscosities [13]

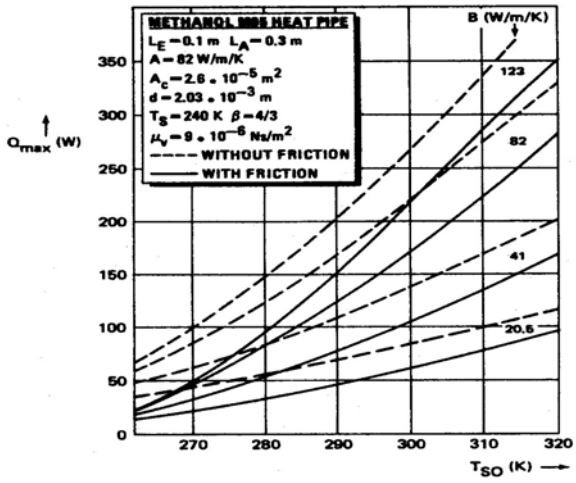

Fig. 16. Maximum power versus source temperature for different evaporator conductance values [13]

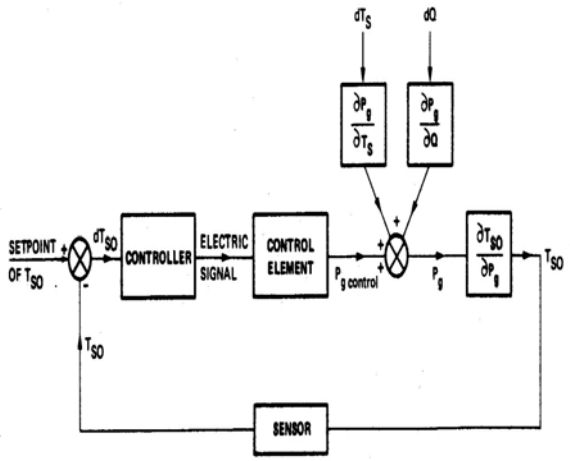

Fig. 17. Feedback control schematic of gas-loaded VCHP (FCHP) [13]

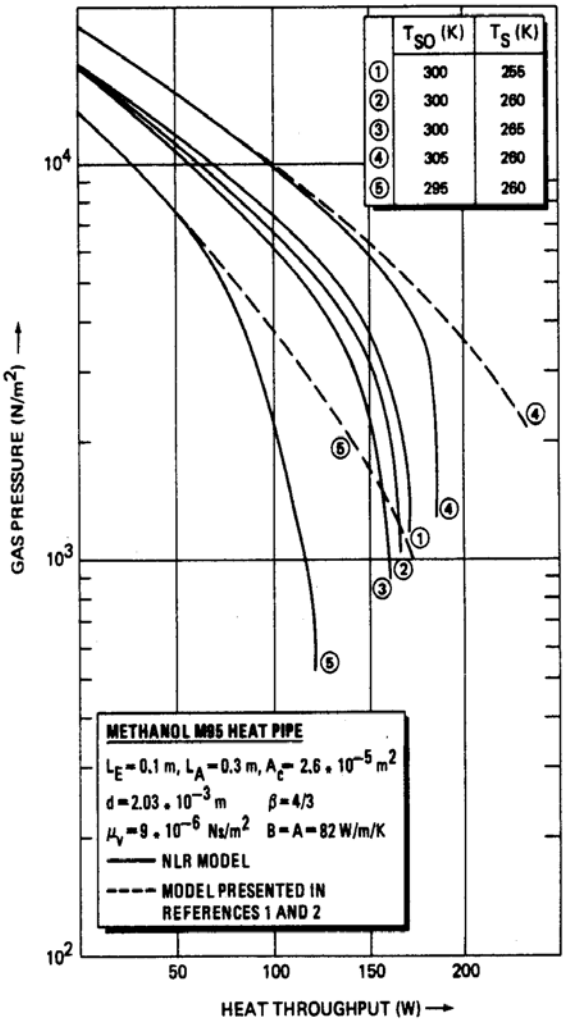

Fig.. 18. Gas pressure downstream of front versus power, for some source and sink temperatures [13]

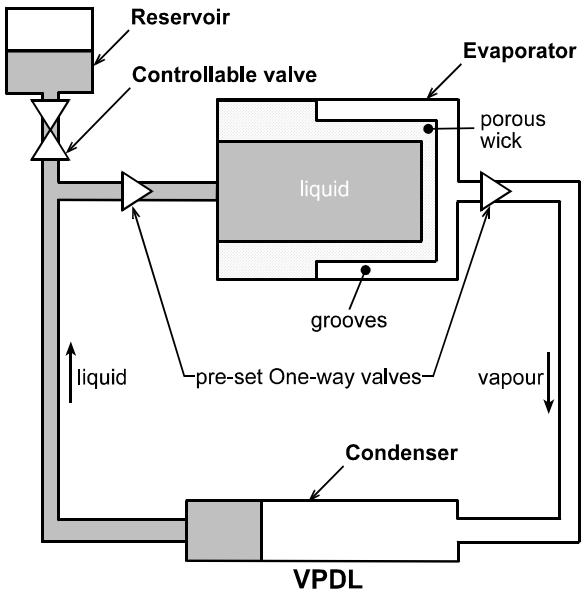

Fig. 19. VPDL schematic [2]

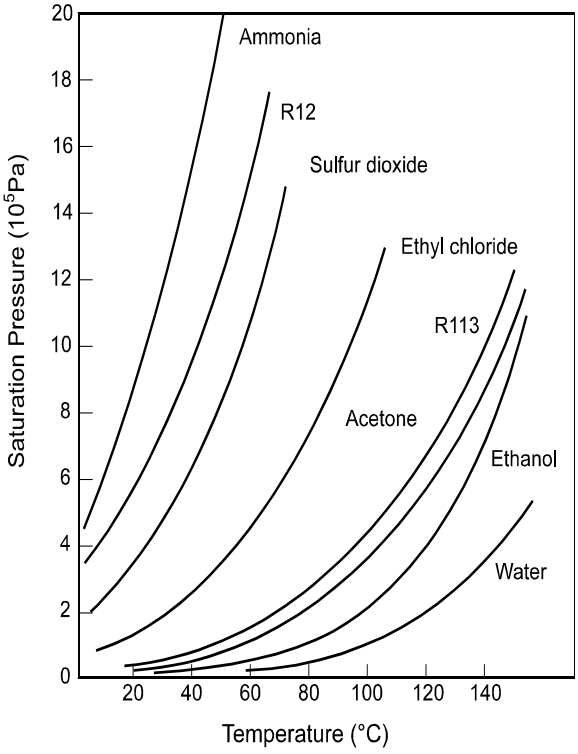

Fig. 20. Vapour pressure versus temperature for various working fluids. [2]

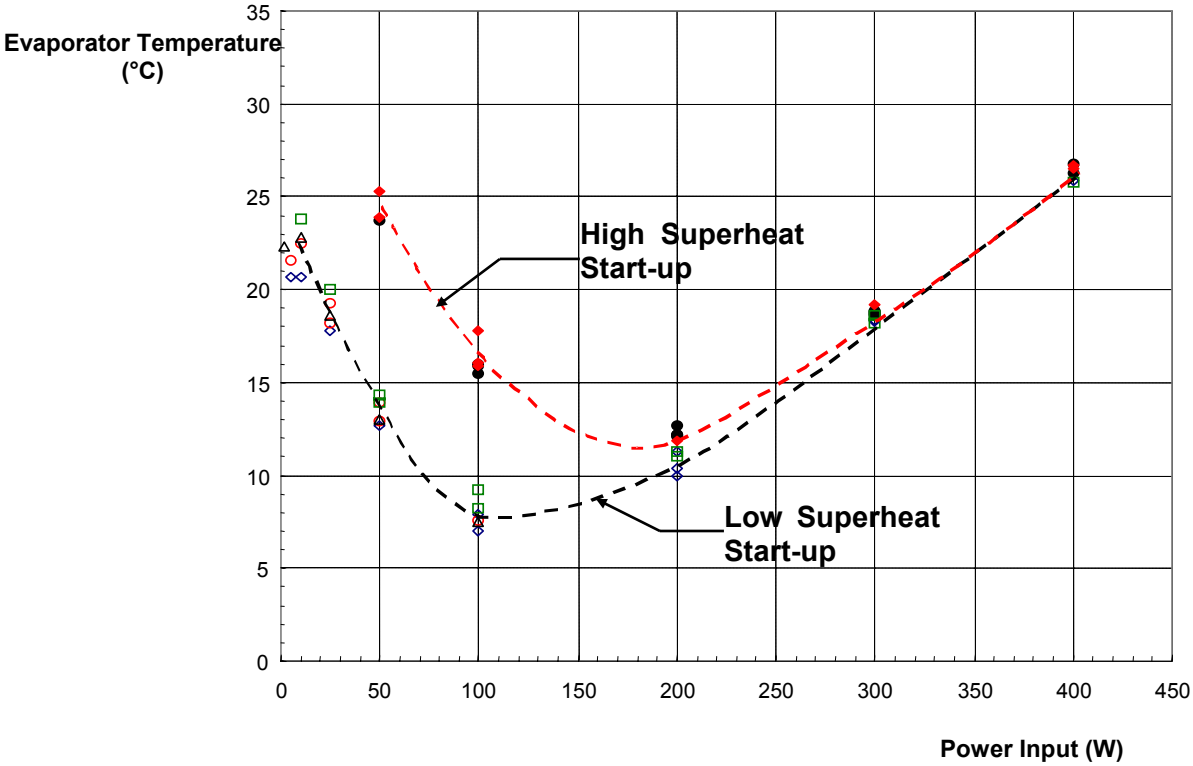

Fig. 21. GLAS LHP performance (courtesy Jentung Ku, NASA-GSFC)